

Tunable non-Markovian dynamics in a collision model: an application to coherent transport

Simone Rijavec^{*,†} and Giuseppe Di Pietra^{*,‡}

Clarendon Laboratory, University of Oxford, Parks Road, Oxford OX1 3PU, United Kingdom

(Dated: May 20, 2024)

We propose a collision model to investigate the information dynamics of a system coupled to an environment with varying degrees of non-Markovianity. We control the degree of non-Markovianity by applying a depolarising channel to a fixed and rigid reservoir of qubits. We characterise the effect of the depolarising channel and apply the model to study the coherent transport of an excitation on a chain of three interacting qubits. We show how the system-environment coupling strength and the degree of non-Markovianity affect the process. Interestingly, in some cases a Markovian environment is preferable to enhance the coherent transport of the excitation.

I. INTRODUCTION

The study of coherent energy transport in quantum systems is of great theoretical and technological importance in physics, chemistry, biology and engineering [1–6]. In photosynthetic systems, long-lived quantum coherence was observed in excitonic energy transfer [7, 8], but its role in the remarkable efficiency of the process has been debated [9–11]. Moreover, the role of the environment in this process has been shown to be complex [12–23].

Nevertheless, photosynthetic systems provide an ideal scenario where recently proposed witnesses of non-classicality could be tested. These witnesses suggest the possibility of indirectly inferring the non-classicality of an unknown system by looking at its capability of creating quantum coherence in a quantum probe [24]. For example, the non-classicality of a generic biopolymer could be inferred by observing the coherence of a photon emitted through the recombination of a delocalised exciton on the polymer [25]. To investigate the possibility of this task, it is essential to understand the mechanism for coherent transport in these systems and clarify the role of the environment in the process.

In this paper, we take an information-theoretic approach to the problem. We propose a *collision model* [26, 27] to study the non-Markovian information dynamics of a chain of qubits interacting with the environment. Differently from other models in the literature [28–35], the system interacts *locally* with the same reservoir qubits and we control the degree of non-Markovianity of the environment by applying a depolarising channel to the reservoir. By changing the intensity of the depolarising effect, we can control the amount of information irretrievably lost by the environment.

We first quantify the degree of non-Markovianity that the depolarising channel induces in the system. Then, we use the collision model to study the coherent transport

of an excitation along a chain of qubits coupled to a *fixed* and *rigid* reservoir of interacting qubits. By changing the degree of non-Markovianity of the reservoir, we can model different types of environments. For example, in an analogy to the Fenna-Matthews-Olson (FMO) photosynthetic complex [36], a Markovian environment could represent the solvent surrounding the complex, while a strongly non-Markovian one could model the phonons of the bacteriochlorophyll molecules that couple to the electronic degrees of freedom responsible for the excitonic transfer.

We show that the transfer of information to the environment plays a crucial role in the coherent transfer of the excitation. The process displays different behaviours depending on the strength of the system-environment coupling. When the system-environment coupling is strong, non-Markovianity dramatically improves the efficiency of coherent transport. Interestingly, when the coupling is weak, a Markovian environment is preferable to enhance the amount of coherence and the coherence time of the excitation.

Our results provide some general insights into how non-Markovian environments affect coherent excitonic transport on a chain. The generality of this model makes it valuable in several fields where energy transport phenomena are relevant. The model also demonstrates how to introduce a control on the degree of non-Markovianity in collision models with a fixed and rigid environment.

II. THE MODEL

The chain. Let us consider an isotropic, 1-dimensional chain of N qubits. We shall call these qubits “system qubits” $S_n, n = 1, \dots, N$. The chain evolves according to a *Heisenberg Hamiltonian* [37]:

$$\hat{H}_{chain} = \frac{1}{2} \sum_{n=1}^N J_{chain}^n \left(\hat{X}_n \hat{X}_{n+1} + \hat{Y}_n \hat{Y}_{n+1} + \hat{Z}_n \hat{Z}_{n+1} \right), \quad (1)$$

with $J_{chain}^n \in \mathbb{R} \ \forall n = 1, \dots, N$ and $\hat{X}_n = \mathbb{I}^{\otimes n-1} \otimes \hat{\sigma}_x \otimes \mathbb{I}^{\otimes N-n+1}$, $\hat{Y}_n = \mathbb{I}^{\otimes n-1} \otimes \hat{\sigma}_y \otimes \mathbb{I}^{\otimes N-n+1}$ and $\hat{Z}_n = \mathbb{I}^{\otimes n-1} \otimes \hat{\sigma}_z \otimes \mathbb{I}^{\otimes N-n+1}$ the Pauli operators describing the

[†] simone.rijavec@physics.ox.ac.uk

[‡] giuseppe.dipietra@physics.ox.ac.uk

* These authors contributed equally to this work

X , Y and Z spin components of the n -th system qubit, respectively. By changing J_{chain}^n , this model can capture different physical systems characterised by different interaction strengths between their constituents. Moreover, the model can be easily generalised to explore other phenomena, such as anisotropies in the chain, next-nearest neighbours coupling, multiple dimensions, and effects of external fields or systems [6].

The environment. We model the environment as a reservoir of N interacting “reservoir qubits” Q_m , $m = 1, \dots, N$. Their interaction is described by a Heisenberg Hamiltonian:

$$\hat{H}_{res} = \frac{1}{2} \sum_{m=1}^N J_{res}^m \left(\hat{X}_m \hat{X}_{m+1} + \hat{Y}_m \hat{Y}_{m+1} + \hat{Z}_m \hat{Z}_{m+1} \right), \quad (2)$$

with coupling constant $J_{res}^m \in \mathbb{R} \forall m = 1, \dots, N$ and \hat{X}_m , \hat{Y}_m , \hat{Z}_m the Pauli operators of the m -th reservoir qubit. Since we are interested in how the information dynamics of the system is affected by a loss of information, we initialise the reservoir qubits in the maximally mixed state

$$\xi = \bigotimes_{m=1}^N \xi_m = \left[\frac{\mathbb{I}}{2} \right]^{\otimes N}, \quad (3)$$

which represents a state containing no information.

We describe the system-environment interactions as *collisions* of each system qubit with its nearest reservoir qubit via a *partial swap* [28]:

$$\hat{P}_m(\eta) = \cos(\eta)\mathbb{I} + i \sin(\eta)\hat{S}_m, \quad (4)$$

where \mathbb{I} is the identity operator, \hat{S}_m the swap operator between the m -th system and reservoir qubit, and $\eta \in [0, \pi/2]$ a parameter that regulates the strength of the interaction. Since $\hat{P}_m(\eta)$ can be written as

$$\hat{P}_m(\eta) = e^{i\eta/2} e^{i\eta/2(\hat{X}_m \hat{X}_m + \hat{Y}_m \hat{Y}_m + \hat{Z}_m \hat{Z}_m)}, \quad (5)$$

all the interactions in the model up to now are fundamentally of the same type.

Non-Markovianity. Since all the interactions considered are unitary and the same reservoir qubits keep interacting with the chain, the model is intrinsically non-Markovian. Unlike other non-Markovian collision models where the reservoir qubits that have interacted with the system are discarded at some point [31–35], we control the *degree* of non-Markovianity of the model by applying a *quantum depolarising channel* to the reservoir qubits after each collision. This allows us to vary the degree of non-Markovianity in a *fixed* and *rigid* environment.

If ρ_{CR} is the state of chain+reservoir, the depolarising channel for a single reservoir qubit can be expressed as:

$$\Delta_{\Omega}^m(\rho_{CR}) = \sum_{i=0}^3 \hat{K}_i^m \rho_{CR} \hat{K}_i^{m\dagger}, \quad (6)$$

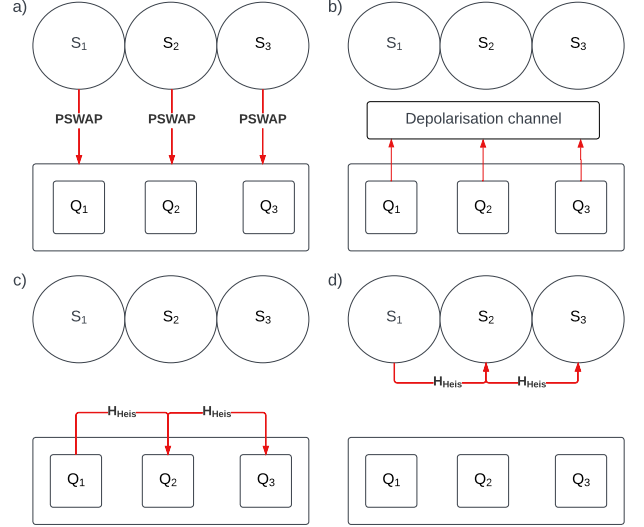


FIG. 1. Four steps of the protocol with three chain qubits and three reservoir qubits. a) exchange phase: each system qubit interacts with its nearest reservoir qubit via a partial swap; b) depolarisation phase: the depolarisation channel is applied to the reservoir qubits; c) transfer via reservoir: unitary evolution of the reservoir qubits with \hat{H}_{res} ; d) transfer via chain: unitary evolution of the system qubits with \hat{H}_{chain} .

where \hat{K}_i^m are the Kraus operators $\hat{K}_0^m := \sqrt{1 - 3\Omega/4} \mathbb{I}_m$, $\hat{K}_1^m := \sqrt{\Omega/4} \hat{X}_m$, $\hat{K}_2^m := \sqrt{\Omega/4} \hat{Y}_m$, $\hat{K}_3^m := \sqrt{\Omega/4} \hat{Z}_m$, and $0 \leq \Omega \leq 1$. Since the \hat{K}_i^m for different m commute, the order in which they are applied is irrelevant.

The parameter Ω controls the amount of information the environment loses. When $\Omega = 0$, $\Delta_0^m(\rho_{CR})$ leaves ρ_{CR} unchanged so that the global evolution of chain+environment is unitary. When $\Omega = 1$, instead, $\Delta_1^m(\rho_{CR})$ re-initialises the m -th reservoir qubit to the maximally mixed state and, if applied to all the reservoir qubits, makes the environment Markovian. It is reasonable to assume that changing $\Omega \in [0, 1]$ allows the exploration of different degrees of non-Markovianity of the environment. In Sec. III A and IV A, we will show how the value of Ω directly relates to a measure of non-Markovianity in the model considered here. Since the degree of non-Markovianity is typically correlated with the environment’s temperature, we call Ω the *effective temperature* of the environment.

The protocol. The protocol consists of four steps (Fig. 1).

1. The system qubits interact with the nearest reservoir qubits via a partial swap (Eq. (4)) with strength η (Fig. 1a). We will call this step the “exchange phase”.
2. The depolarisation channel is applied to the reser-

voir qubits (Fig. 1b). This step controls the degree of non-Markovianity of the environment. We will call this step the “depolarisation phase”.

3. The reservoir qubits evolve according to the Hamiltonian of Eq. (2) for a time interval Δt (Fig. 1c). We will call this step the “transfer via reservoir”.
4. The system qubits evolve according to the Hamiltonian of Eq. (1) for a time interval Δt (Fig. 1d). We will call this step the “transfer via chain”.

All the steps of the protocol can be repeated indefinitely.

III. METHODS

In this section, we start by discussing the measure of non-Markovianity we use to characterise the effect of the depolarising channel. Then, we show how our model can be applied to study the coherent transport of an excitation along the chain.

A. Quantifying the degree of non-Markovianity

The measure of non-Markovianity we use is the one proposed in [38]. Given two initial states of the system $\rho_1(0)$ and $\rho_2(0)$, the degree of non-Markovianity under the action of a dynamical map is measured as [38]:

$$\mathcal{N} = \max_{\{\rho_1(0), \rho_2(0)\}} \int_{\Sigma_+} \frac{d}{dt} D(\rho_1(t), \rho_2(t)) dt, \quad (7)$$

where Σ_+ is the union of all subsets where $\frac{d}{dt} D(\rho_1(t), \rho_2(t)) > 0$ and

$$D(\rho_1(t), \rho_2(t)) = \frac{1}{2} \|\rho_1(t) - \rho_2(t)\|_1, \quad (8)$$

is the trace distance between $\rho_1(t)$ and $\rho_2(t)$. Since in this work we consider a discrete process, we use a discretised version of Eq. (7) [38]:

$$\mathcal{N} = \max_{\{\rho_{1,0}, \rho_{2,0}\}} \sum_{n \in \Sigma_+} (D(\rho_{1,n}, \rho_{2,n}) - D(\rho_{1,n-1}, \rho_{2,n-1})), \quad (9)$$

where the summation is taken on all values of n such that $D(\rho_{1,n}, \rho_{2,n}) - D(\rho_{1,n-1}, \rho_{2,n-1}) > 0$, $\rho_{1,n}$ is the state of the system at the end of the n -th step obtained by tracing out the environment, and the maximisation is performed over all pairs of initial states $\{\rho_{1,0}, \rho_{2,0}\}$.

To illustrate the effect of the depolarising channel on the degree of non-Markovianity, we first restrict to a model with one system qubit and one reservoir qubit (1x1). We measure the non-Markovianity of this model by maximising Eq. (9) over all the pairs of initial system states prepared in the following way:

$$\rho_{k,0} = \frac{1}{2} \begin{pmatrix} 1 + r_k \cos(\theta_k) & r_k \sin(\theta_k) e^{-i\Phi_k} \\ r_k \sin(\theta_k) e^{i\Phi_k} & 1 - r_k \cos(\theta_k) \end{pmatrix}, \quad (10)$$

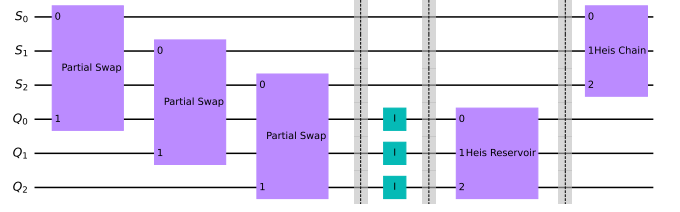


FIG. 2. Quantum circuit implementing an iteration of the protocol in our model. The three PSWAP gates implement the exchange phase. A depolarising error is associated with each identity gate to implement the depolarisation phase. The two final gates implement the unitary evolutions with the Hamiltonians \hat{H}_{res} and \hat{H}_{chain} of the transfer phases.

with $r_k \in [0, 1]$, $\theta_k \in [0, \pi]$, and $\phi_k \in [0, 2\pi]$, for $k = 1, 2$.

The maximisation procedure becomes too complicated with a higher number of qubits. In this case, we use some of the insights on the states maximising Eq. (9) drawn from the 1x1 case to choose a suitable pair of initial states.

B. Application to coherent transport

We apply the model described above to study the coherent transport of an excitation along the chain. We represent an excitation localised on the first qubit as

$$\rho_C(0) = |100\dots 0\rangle \langle 100\dots 0|, \quad (11)$$

in the Hilbert space $\mathcal{H}_{S_1} \otimes \dots \otimes \mathcal{H}_{S_N}$. Applying the protocol described above, the excitation spreads through the chain and the environment. After repeating the protocol k times we trace out the environment and extract the coherence between the first and last qubit of the chain $\rho_C^{1,N}$. We take $|\rho_C^{1,N}|$ as an indicator of the coherent transport efficiency across the chain.

For simplicity, we consider a model with three chain qubits. Fig. 2 shows how an iteration of the protocol can be implemented as a quantum circuit in Qiskit [39]. The exchange phase consists of a sequence of local unitaries $\hat{P}(\eta)$ as in Eq. (4) for each of the system qubits S_i ; the depolarisation phase is implemented as a depolarising noise model on the identity gate, which applies the quantum channel of Eq. (6); the transfer phases are implemented as unitaries on system and reservoir with a time step $\Delta t = 0.01$. We choose $J_{chain}^n = J_{chain} = 10$, $\forall n$ and $J_{res}^m = J_{res} = 1$, $\forall m$. This choice represents a scenario where the chain is the most efficient medium for the propagation of the excitation.

We first apply the protocol two times and study how $|\rho_C^{1,3}|$ varies for different values of η and Ω . This leaves enough time for the excitation to reach the last qubit of the chain, passing through the intermediate qubit, and is sufficient to obtain some general insights on how the environment affects coherent transport. Then, we select some values of η and Ω and repeat the protocol with more iterations. The results show how $|\rho_C^{1,3}|$ varies over time.

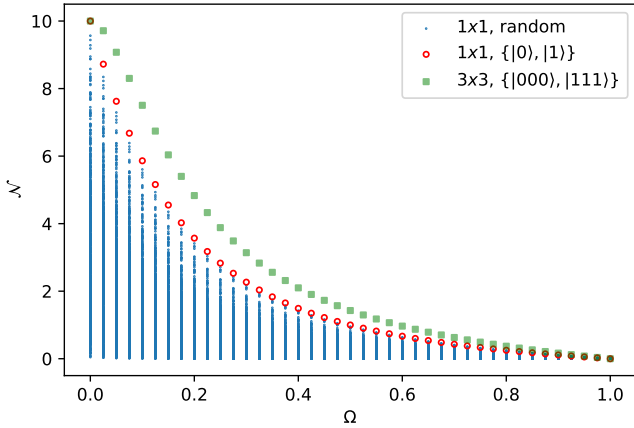


FIG. 3. Degree of non-Markovianity \mathcal{N} as a function of Ω for two different models. \mathcal{N} is calculated over 20 time steps with $\eta = \pi/2$. The blue circles correspond to values of \mathcal{N} calculated with 1000 randomly generated pairs of initial system states in the 1x1 model. The red circles are the values of \mathcal{N} obtained with the initial states $|0\rangle$ and $|1\rangle$. The green squares correspond to the values of \mathcal{N} for the 3x3 model with initial states $|000\rangle$ and $|111\rangle$.

IV. RESULTS

Here, we present the results obtained from the simulations of the collision model with the methods described in Sec. III A and III B.

A. Non-Markovianity

In Fig. 3, we plot the degree of non-Markovianity \mathcal{N} induced by our protocol in two models with different numbers of qubits. The circles refer to a model with one system qubit and one reservoir qubit (1x1), and the squares to the model with three system qubits and three reservoir qubits (3x3). We have calculated \mathcal{N} over 20 temporal steps with $\eta = \pi/2$ for different values of Ω .

The blue circles correspond to values of \mathcal{N} for 1000 randomly generated pairs of initial states of the system in the 1x1 model. The red circles correspond to the initial states $|0\rangle$ and $|1\rangle$. The graph provides strong numerical evidence that $|0\rangle$ and $|1\rangle$ maximise \mathcal{N} in Eq. (9). During the course of the simulations, we noticed that any two antipodal states on the Bloch sphere would maximise \mathcal{N} . This observation leads us to consider $|000\rangle$ and $|111\rangle$ as good candidates to maximise \mathcal{N} in the 3x3 model. The green squares correspond to values of \mathcal{N} for this pair of initial states and show a behaviour consistent with the 1x1 case. Due to the computational demand of simulating the 3x3 model with many different initial states, we consider only the pair $\{|000\rangle, |111\rangle\}$. The green squares can then be interpreted as a lower bound on the non-Markovianity of the 3x3 model, although we conjecture that they maximise it.

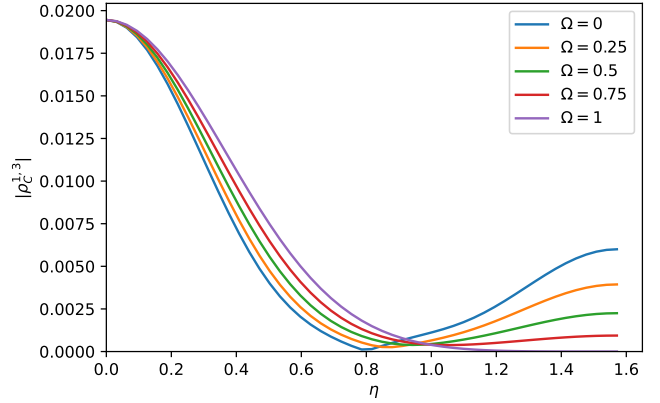


FIG. 4. Coherence element $|\rho_C^{1,3}|$ as a function of the system-environment coupling η for different values of the effective temperature Ω when $J_{chain} = 10$, $J_{res} = 1$.

Fig. 3 shows that the parameter Ω directly relates to the degree of non-Markovianity \mathcal{N} of the models. \mathcal{N} is maximal for $\Omega = 0$, that is when the evolution of system+reservoir is unitary. \mathcal{N} monotonically decrease with higher values of Ω and becomes null for $\Omega = 1$, i.e. when the reservoir is completely depolarised at each step. The results are similar for the 1x1 and 3x3 models and show that Ω is a good parameter to control the degree of non-Markovianity of the model.

B. Coherent transport

In Fig. 4 we plot $|\rho_C^{1,3}|$ after two time steps as a function of η for different values of Ω . The value of $|\rho_C^{1,3}|$ for $\eta = 0$ represents the coherence between the first and last qubits in the absence of system-environment interaction. This value is obviously unaffected by the value of Ω .

Moving on to values of $\eta < \frac{\pi}{4}$, which we shall call the “weak coupling” regime, we observe a decrease in $|\rho_C^{1,3}|$, meaning that system-environment interactions lead to less efficient coherent transport. Interestingly, for the same η , higher values of Ω lead to higher coherence, meaning that a *Markovian* environment is preferable to a non-Markovian one.

Approaching higher values of η , the coherence decreases monotonically for $\Omega = 1$ while for $\Omega \neq 1$ it reaches a minimum and then increases again. The position of the minima depends on the value of Ω : the more Markovian the environment, the stronger the system-environment coupling must be to minimise the coherence. In the “strong coupling” regime, we observe a considerable *coherence revival*, with lower values of Ω associated with higher rebounds.

So far, we have considered how the coherence is affected by η and Ω after two iterations of the protocol. To check whether these results are consistent with the behaviour of the system over longer time scales, in Fig.

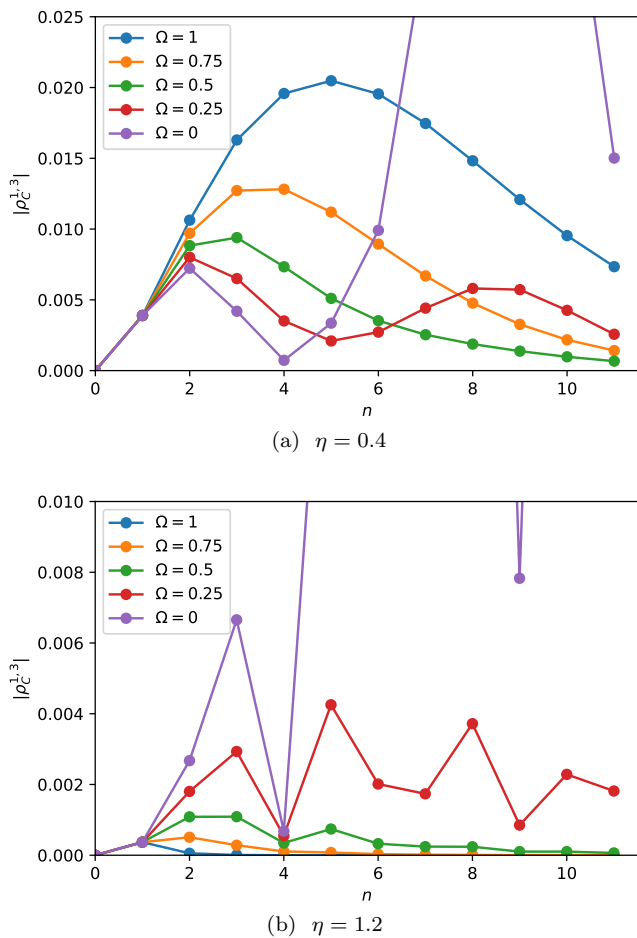


FIG. 5. Coherence element $|\rho_C^{1,3}|$ over multiple iterations of the protocol for different values of Ω . The case $\Omega = 0$ represents the *unrealistic* scenario of a fully unitary evolution. In this case, the coherence oscillates wildly, so the vertical axis has been truncated to improve the visibility of the graphs.

we plot $|\rho_C^{1,3}|$ as a function of the number of iterations of the protocol n for different values of Ω . We consider two cases: a) $\eta = 0.4$ (weak coupling regime), and b) $\eta = 1.2$ (strong coupling regime).

Starting with Fig. 5a, we observe that the first peak of $|\rho_C^{1,3}|$ is consistent with the results of Fig. 4: a *Markovian* environment results in greater coherence. Excluding the oscillatory behaviour of the ideal case $\Omega = 0$ (no information loss), at later times the coherence is suppressed, with higher values of Ω generally associated with longer coherence times. This reinforces the interesting observation that a Markovian environment better assists coherent transport in the weak coupling regime.

Consistently with Fig. 4, the situation is flipped in the strong coupling regime. In Fig. 5b we observe that the coherence is immediately suppressed for higher values of Ω while it is more persistent for highly non-Markovian environments.

Overall, we can conclude that non-Markovianity improves the coherent transport for strong system-

environment couplings but hinders it if the coupling is weak. In the weak coupling regime, a Markovian environment enhances both the amount of coherence and the coherence time of the excitation. Note that these two mechanisms may not be mutually exclusive. For example, in the FMO photosynthetic complex, the electronic degrees of freedom of the bacteriochlorophyll molecules (the chain in our model) can couple both to the phonons of the molecular environment (non-Markovian) and to an external thermal bath (Markovian environment). Our results capture both of these situations, suggesting that the coexistence of a weakly coupled thermal bath and a strongly coupled non-Markovian environment may determine an optimal condition for coherent excitonic transport.

V. CONCLUSIONS

In this work, we have proposed a collision model that allows direct control of the environmental degree of non-Markovianity. We have fixed the number and geometry of the reservoir qubits and induced information loss by applying depolarising channels on them. We have characterised the effect of the depolarising channel by measuring the degree of non-Markovianity of the model, showing how the intensity of the former directly relates to the latter.

We have applied our model to study the quantum coherent excitonic transport on a chain of interacting qubits coupled to an environment. Our model permits the exploration of how different regimes of non-Markovianity and system-environment coupling affect coherent transport. Studying this aspect is important in photosynthetic complexes, where the electronic degrees of freedom responsible for the coherent transport of an exciton can couple to both Markovian (e.g. solvent) and non-Markovian (phonons) environments. Our results show that a non-Markovian environment aids coherent transport only in the strong system-environment coupling regime, while a *Markovian* environment is surprisingly preferable in the weak coupling regime.

This work provides some general insights into how non-Markovianity affects coherent excitonic transport, avoiding the complications that arise from accurately modelling a real complex physical system. Its generality makes it suitable for applications to any quantum processes whose understanding involves the exchange of information between the system and the environment. The model could also be easily adapted to study more specific systems. For example, one could expand the dimensions of the chain and the environment, use more realistic Hamiltonians, or use two different environments, one Markovian and one non-Markovian. These generalisations could be relevant to inform the development of novel technological applications. The model could also be implemented on current quantum computer [40]. We leave these investigations for future work.

ACKNOWLEDGMENTS.

We thank Maria Violaris, Vlatko Vedral and Chiara Marletto for their sharp comments and fruitful discus-

sions on this manuscript. S.R. thanks the Fondazione “Angelo Della Riccia”. G.D.P. thanks the Clarendon Fund and the Oxford-Thatcher Graduate Scholarship for supporting this research.

-
- [1] D. V. Alexandrov and A. Y. Zubarev, *Philosophical Transactions of the Royal Society A: Mathematical, Physical and Engineering Sciences* **379**, 20200301 (2021).
 - [2] D. V. Alexandrov and A. Y. Zubarev, *Philosophical Transactions of the Royal Society A: Mathematical, Physical and Engineering Sciences* **380**, 20210366 (2022).
 - [3] S. Lloyd, *J. Phys.: Conf. Ser.* **302**, 012037 (2011).
 - [4] Y. Kim, F. Bertagna, E. M. D’Souza, D. J. Heyes, L. O. Johannissen, E. T. Nery, A. Pantelias, A. Sanchez-Pedreño Jimenez, L. Slocombe, M. G. Spencer, J. Al-Khalili, G. S. Engel, S. Hay, S. M. Hingley-Wilson, K. Jeevaratnam, A. R. Jones, D. R. Kattnig, R. Lewis, M. Sacchi, N. S. Scrutton, S. R. P. Silva, and J. McFadden, *Quantum Reports* **3**, 80 (2021).
 - [5] M. Müller, S. Diehl, G. Pupillo, and P. Zoller, in *Advances In Atomic, Molecular, and Optical Physics*, Advances in Atomic, Molecular, and Optical Physics, Vol. 61, edited by P. Berman, E. Arimondo, and C. Lin (Academic Press, 2012) pp. 1–80.
 - [6] A. Civolani, V. Stanzione, M. L. Chiofalo, and J. Yago Malo, *Entropy* **26**, 20 (2024).
 - [7] G. S. Engel, T. R. Calhoun, E. L. Read, T.-K. Ahn, T. Mančal, Y.-C. Cheng, R. E. Blankenship, and G. R. Fleming, *Nature* **446**, 782 (2007).
 - [8] G. Panitchayangkoon, D. Hayes, K. A. Fransted, J. R. Caram, E. Harel, J. Wen, R. E. Blankenship, and G. S. Engel, *Proceedings of the National Academy of Sciences* **107**, 12766 (2010).
 - [9] D. M. Wilkins and N. S. Dattani, *J. Chem. Theory Comput.* **11**, 3411 (2015).
 - [10] H.-G. Duan, V. I. Prokhorenko, R. J. Cogdell, K. Ashraf, A. L. Stevens, M. Thorwart, and R. J. D. Miller, *Proceedings of the National Academy of Sciences* **114**, 8493 (2017).
 - [11] M.-J. Tao, N.-N. Zhang, P.-Y. Wen, F.-G. Deng, Q. Ai, and G.-L. Long, *Science Bulletin* **65**, 318 (2020).
 - [12] H. Lee, Y.-C. Cheng, and G. R. Fleming, *Science* **316**, 1462 (2007).
 - [13] M. Mohseni, P. Rebentrost, S. Lloyd, and A. Aspuru-Guzik, *The Journal of Chemical Physics* **129**, 174106 (2008).
 - [14] P. Rebentrost, M. Mohseni, I. Kassal, S. Lloyd, and A. Aspuru-Guzik, *New J. Phys.* **11**, 033003 (2009).
 - [15] P. Rebentrost, M. Mohseni, and A. Aspuru-Guzik, *J. Phys. Chem. B* **113**, 9942 (2009).
 - [16] J. Strümpfer and K. Schulten, *J Chem Phys* **134**, 095102 (2011).
 - [17] P. Rebentrost and A. Aspuru-Guzik, *The Journal of Chemical Physics* **134**, 101103 (2011).
 - [18] V. Butkus, D. Zigmantas, L. Valkunas, and D. Abramavicius, *Chemical Physics Letters* **545**, 40 (2012).
 - [19] S. Huelga and M. Plenio, *Contemporary Physics* **54**, 181 (2013).
 - [20] R. Tempelaar, T. L. C. Jansen, and J. Knoester, *J. Phys. Chem. B* **118**, 12865 (2014).
 - [21] A. Halpin, P. J. M. Johnson, R. Tempelaar, R. S. Murphy, J. Knoester, T. L. C. Jansen, and R. J. D. Miller, *Nature Chem* **6**, 196 (2014).
 - [22] H.-G. Duan, P. Nalbach, V. I. Prokhorenko, S. Mukamel, and M. Thorwart, *New J. Phys.* **17**, 072002 (2015).
 - [23] M. Reppert and P. Brumer, *The Journal of Chemical Physics* **149**, 234102 (2018).
 - [24] G. Di Pietra and C. Marletto, *J. Phys. A: Math. Theor.* **56**, 265305 (2023).
 - [25] G. Di Pietra, V. Vedral, and C. Marletto, *arXiv:2306.12799 [quant-ph]* (2023).
 - [26] S. Campbell and B. Vacchini, *EPL* **133**, 60001 (2021).
 - [27] F. Ciccarello, S. Lorenzo, V. Giovannetti, and G. M. Palma, *Physics Reports Quantum collision models: Open system dynamics from repeated interactions*, **954**, 1 (2022).
 - [28] M. Ziman, P. Štelmachovič, V. Bužek, M. Hillery, V. Scarani, and N. Gisin, *Phys. Rev. A* **65**, 042105 (2002).
 - [29] M. Ziman, P. Štelmachovič, and V. Bužek, *Open Syst Inf Dyn* **12**, 81 (2005).
 - [30] M. Ziman and V. Bužek, *Phys. Rev. A* **72**, 022110 (2005).
 - [31] F. Ciccarello, G. M. Palma, and V. Giovannetti, *Phys. Rev. A* **87**, 040103 (2013).
 - [32] R. McCloskey and M. Paternostro, *Phys. Rev. A* **89**, 052120 (2014).
 - [33] S. Kretschmer, K. Luoma, and W. T. Strunz, *Phys. Rev. A* **94**, 012106 (2016).
 - [34] Z.-X. Man, Y.-J. Xia, and R. Lo Franco, *Phys. Rev. A* **97**, 062104 (2018).
 - [35] T. Saha, A. Das, and S. Ghosh, *New J. Phys.* **26**, 023011 (2024).
 - [36] B. W. Matthews, R. E. Fenna, M. C. Bolognesi, M. F. Schmid, and J. M. Olson, *Journal of Molecular Biology* **131**, 259 (1979).
 - [37] A. Kay, *Int. J. Quantum Inform.* **08**, 641 (2010).
 - [38] H.-P. Breuer, E.-M. Laine, and J. Piilo, *Phys. Rev. Lett.* **103**, 210401 (2009).
 - [39] Qiskit contributors, *Qiskit: An open-source framework for quantum computing* (2023).
 - [40] S. Leontica, F. Tennie, and T. Farrow, *Commun Phys* **4**, 1 (2021).